

Improved load frequency control in dual-area hybrid renewable power systems utilizing PID controllers optimized by the salp swarm algorithm

Pushpa Sreenivasan¹, Lakshmi Dhandapani¹, Shanthi Natarajan², Arul Doss Adaikalam³,
Amudhapriya Sivakumar⁴

¹Department of Electrical and Electronics Engineering, Faculty of Engineering and Technology, AMET University, Tamilnadu, India

²Department of Electrical and Electronic Engineering, Sri Sai Ram Institute of Technology, Tamilnadu, India

³Department of Electrical and Electronic Engineering, Chennai Institute of Technology, Tamilnadu, India

⁴Department of Electrical and Electronic Engineering, Panimalar Engineering College, Tamilnadu, India

Article Info

Article history:

Received Nov 11, 2023

Revised Mar 5, 2024

Accepted Apr 9, 2024

Keywords:

Dynamic renewable energy sources

Load frequency control

Optimization methods

Power system control

Salp swarm algorithm

SSA-PID controller

ABSTRACT

In this study, we utilize the salp swarm algorithm (SSA) to optimize proportional integral derivative (PID) controller gains for load frequency control (LFC) in a multi-area hybrid renewable nonlinear power system. Incorporating generation rate constraints and dead-bands into the governor model, we examine system nonlinearities. Performance evaluation employs both single- and multi-objective functions, with actual sun irradiation data validating SSA-PID controllers' efficacy in managing renewable energy source uncertainties. Comparing with alternative optimization techniques across various operational scenarios reveals the SSA-PID controller's 15% improvement in dynamic response time. The findings suggest SSA enhances LFC dynamic response in hybrid renewable power systems, with potential generalizability. These results underscore SSA's utility in addressing system complexities, offering implications for improved stability and efficiency across renewable energy integration scenarios.

This is an open access article under the [CC BY-SA](https://creativecommons.org/licenses/by-sa/4.0/) license.



Corresponding Author:

Lakshmi Dhandapani

Department of Electrical and Electronics Engineering, Faculty of Engineering and Technology

AMET University

East Coast Road 135, Kanathur, 603112, Tamilnadu, India

Email: lakshmiee@gmail.com

1. INTRODUCTION

This paper presents a novel solution to the load frequency control (LFC) issue in contemporary power networks that use renewable energy sources. The method optimizes proportional integral derivative (PID) controllers made especially for multi-area hybrid renewable power systems by using the salp swarm algorithm (SSA). The authors contribute significantly by introducing SSA as an efficient alternative to existing meta-heuristic optimization algorithms, drawing inspiration from salps' collective behavior for adaptability to nonlinear dynamics in renewable energy-integrated power systems [1]–[3]. Unlike conventional strategies discussed in earlier studies, including novel approach to SSA-PID controller design that combines nonlinearity using a governor model with a dead-band and a generation rate constraint, utilizing genetic algorithm and particle swarm optimization [4]–[10]. This innovation aims to enhance LFC dynamic responses, filling a critical gap in existing works.

The central focus is on addressing LFC challenges in multi-area hybrid renewable power systems, with specific design goals including incorporating nonlinearity, achieving efficient PID tuning with SSA, and

assessing controller effectiveness using real sun irradiation data to account for variability in renewable energy sources. The studies [11]–[15] anticipate improved performance and stability in load frequency control, contributing significantly to control strategy evolution for renewable energy-integrated power systems. This work represents a notable advancement in developing robust and adaptive solutions for dynamic challenges posed by renewable energy sources in power system control [16]–[20].

2. MATHEMATICAL MODELLING OF LOAD FREQUENCY CONTROL

The study examines a two-area hybrid renewable system with a 2000 MW capacity and 1000 MW load per area, operating at 50 Hz. Mathematical transfer functions detail governors, turbines, reheaters, and the power system for control strategy design [21]–[23]. Modelling of two area system shown in Figure 1 presents a two-area interconnected hybrid renewable system used in this investigation.

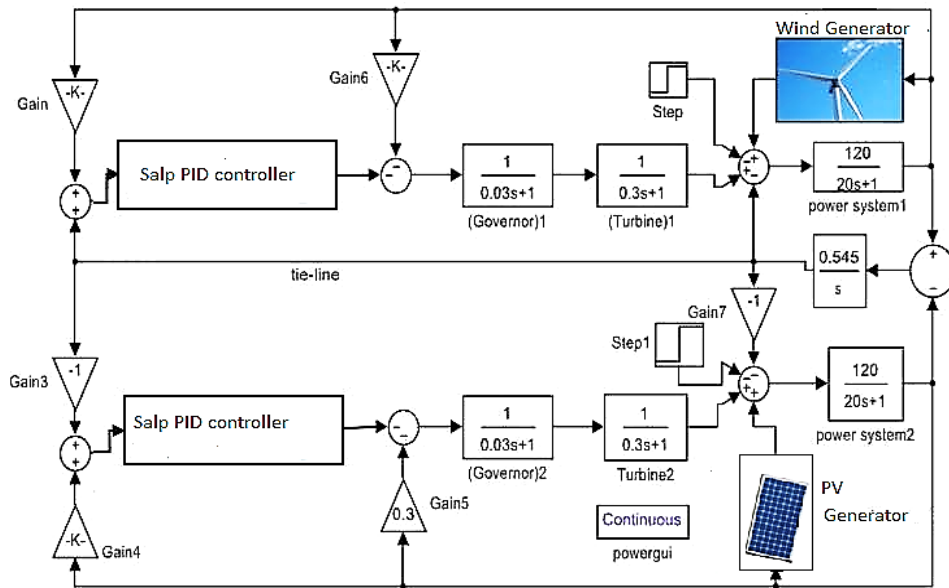


Figure 1. Modelling of two area system

2.1. Thermal power plant

The parameters of the model consist of R, B, Tg, Tt, Th, Tp, Kh, Kp, and T12. Adopting a 0.0006 p.u. dead band is in line with AIEE-ASME standards and represents industry best practices. In order to balance robustness against noise and susceptibility to system fluctuations, this dead band value was selected. The controller's performance and stability under various operating situations also play a role in its selection. Additionally, investigating how various dead band values affect system behavior may shed light on the best methods for parameter tuning load frequency control (LFC) in hybrid renewable energy systems [24], [25]. As a result, this decision demonstrates a diligent attempt to uphold standards while also taking into account real-world applications and potential research avenues, and a 5% per minute governor rate constraint (GRC) in the turbine model influences LFC system performance. Frequency (F) and tie line power changes (P_{tie}) are denoted. The (1) can be used to calculate the tie line power (P_{tie}) moved from area-1 to area-2.

$$P_{tie} = \frac{|V_1||V_2| \sin(\delta_1 - \delta_2)}{X_{12}} \tag{1}$$

In this context, X₁₂ symbolizes the reactance of the tie line, while δ₁ and δ₂ represent the power angles in their respective regions. Furthermore, |V₁| and |V₂| indicate the voltage magnitudes in area-1 and area-2. For an accurate model of P_{tie}, it is essential to consider factors influencing |V₁| and |V₂|. This consideration can be expressed through (2) and (3), after performing the necessary partial differentiations.

$$\Delta P_{tie} = \frac{\partial P_{tie} \Delta |V_1|}{\partial |V_1|} + \frac{\partial P_{tie} \Delta |V_2|}{\partial |V_2|} + \frac{\partial P_{tie} \Delta |\delta_1 - \delta_2|}{\partial |\delta_1 - \delta_2|} \tag{2}$$

$$\Delta P_{tie} = T_1 \Delta |V_1| + T_2 \Delta |V_2| + T_{12} \Delta |\delta_1 - \delta_2| \quad (3)$$

Here, T1 and T2 are coefficients determined as (4) and (5).

$$T_1 = \frac{|V_2^o| \sin(\delta_1^o - \delta_2^o)}{(X_{12})} \quad (4)$$

$$T_2 = \frac{|V_1^o| \sin(\delta_1^o - \delta_2^o)}{(X_{12})} \quad (5)$$

2.2. Wind farm

This mathematical equation provides the expression for the mechanical power (Pm) extracted from wind, as in (6).

$$P_m = 0.5 C_p \rho \pi r^2 V_w^3 (\lambda, \beta) \quad (6)$$

Here, ρ represents where air density is denoted by ρ , λ represents the tip speed ratio, β is the blade pitch angle, r stands for the blade radius, V_w signifies the wind speed, and C_p is computed using (7).

$$\begin{aligned} C_p &= 0.5(\lambda i - 0.022\beta^2 - 5.6)e^{-0.17\lambda i} \\ \lambda &= (\omega_B R / V\omega) \\ \lambda i &= (3600R) / (1609\lambda) \end{aligned} \quad (7)$$

Additionally, the calculation of the tip speed ratio (λ) is determined by the formula provided in (7). In this context, ω_B represents the blade speed, R denotes the blade radius, λi represents the tip speed ratio. The transfer function in the mathematical model of the wind induction generator has a gain of unity and a time constant of 0.3 seconds. This model is utilized for MPPT conditions, where the pitch controller is employed.

2.3. PV system

PV modules are represented in this research project, a mathematical model is employed, utilizing a single-diode PV model. The model's ability to blend accuracy and simplicity is what led to this choice. The PV module's nonlinear I-V characteristic can be expressed as in (8).

$$I = I_{pv} - I_o \left(\exp\left(\frac{V + R_s I}{a V_i}\right) - 1 \right) - \frac{V + R_s I}{R_p} \quad (8)$$

The investigation incorporates real data obtained from an operational PV power plant, specifically employing a KC200GT solar PV module within a 50 MW large-scale PV system. The DC-DC converter and grid-side inverter circuits that make up the power electronic interface circuits, have unity gain transfer functions and a 10 ms time constant. MATLAB/Simulink is used to implement the integrated hybrid renewable power system's whole model.

3. FORMULATING PROBLEMS AND THE SSA CODE

The power system's LFC loop is used in this study, and a popular PID controller with the following design variables is used: derivative filter coefficient (N), proportional gain (k_p), integral gain (k_i), and derivative gain (k_d). The transfer function of the PID controller is formulated for analysis, as in (9).

$$K_p + K_i(1/S) + K_d(N/1 + N.(1/S)) \text{ equals } I_{GC}(S) \quad (9)$$

In LFC system design, the choice of the objective function significantly influences power system dynamic responses. Common integral criteria, including integral square error (ISE) using (10), integral time square error (ITSE) using (11) integral absolute error (IAE) using (12), and integral of time absolute error (ITAE) as in (13), serve to define the objective function. These criteria balance factors like overshoot, settling time, and time-varying parameters, applied either individually or as multi-objective functions in the study.

$$ISE = t_s \int_0 (\Delta F_1 + \Delta F_2 + \Delta P_{tie2}) dt \quad (10)$$

$$ITSE = t_s \int_0 t. (\Delta F_1 + \Delta F_2 + \Delta P_{tie2}) dt \quad (11)$$

$$IAE = ts \int_0 (\left| \Delta F1 \right| + \left| \Delta F2 \right| + \left| \Delta P_{tie2} \right|) dt \quad (12)$$

$$ITAE = ts \int_0 (t \left| \Delta F1 \right| + \left| \Delta F2 \right| + \left| \Delta P_{tie2} \right|) dt \quad (13)$$

Subjected to the constraint on PID gains, as in (14) and (15).

$$K_{p^{m,i,d} \min} \leq K_{p^{m,i,d}} \leq K_{p^{m,i,d} \max} \text{ for all } m \in \frac{N_{PID} \left(\frac{1}{2\pi} \right) 2\pi \int_0 d\theta}{a+b\sin\theta} = \frac{1}{\sqrt{a^2+b^2}} \quad (14)$$

$$N^{m \min} \leq N^m \leq N^{m \max} \text{ for all } m \in N_{PID} \quad (15)$$

Simulation time, " t_s ," corresponds to $N^{m \min}$ and $N^{m \max}$ the filter coefficients, given in (15), lower and upper bounds for the m th PID controller. The lower and upper bounds for the proportional, integral, and derivative gains of the m th PID controller are also established by $K_{p^{m,i,d} \min}$, and $K_{p^{m,i,d} \max}$, using (14). The SSA optimization aims to minimize a specified function, obtaining optimal controller parameters for diverse power system operating conditions.

3.1. The SSA code

SALP, inspired by spider behavior, is a metaheuristic optimization algorithm with cooperative hunting and local population maintenance for solving optimization problems in various domains. The step-by-step procedure of SALP algorithm are given below:

- Step1: Initialize the population of candidate solutions (spiders) randomly or using some other suitable method.
- Step 2: Based on the optimization problem's objective function, assess each spider's fitness within the population.
- Step 3: Identify the global best spider (the one with the best fitness value) from the population.
- Step 4: Update the position of each spider based on its own previous position and the position of the global best spider.
- Step 5: Update the local population for each spider based on its position and the positions of its neighbor's.
- Step 6: Evaluate the fitness of the new candidate solutions (updated spiders).
- Step7: Compare the fitness of the updated spiders with the current population, and replace the worst individuals with the updated spiders to maintain the population size.
- Step 8: For a predetermined number of iterations or until a termination condition is satisfied, repeat steps 3 through 7 again.

The algorithm utilizes local populations around each spider to efficiently explore the solution space and maintain a balance between exploration and exploitation. Through iterative position updates and information exchange among local populations, the algorithm strives to converge towards improved solutions overtime.

$$X_j^1 = \{ F_j + C_1((HL_j - LL_j)C_2 + LL_j) \text{ for all } C_3 < 0.5$$

$$F_j + C_1((HL_j - LL_j)C_2 + LL_j) \text{ for all } C_3 \geq 0.5 \} \quad (16)$$

$$C_1 = 2 \cdot \text{Exp}(-(4k/\text{Max_Iter})^2) \quad (17)$$

$$C_2 = \text{rand}(\dots) \text{ and } C_3 = \text{rand}(\dots) \quad (18)$$

$$X_j^i = 1/2(X_{ij}X_j^i + X_j^{i-1}) \text{ for all } 2 \leq i \leq \text{max_Iter} \quad (19)$$

The position of the food source in the j th dimension is denoted by the formula F_j , can use (16), constrained by upper (HL_j) and lower (LL_j) bounds. The position updates are determined by randomly distributed numbers C_2 and C_3 , as in (18), the iteration counter k , and Max_Iter , with the critical factor C_1 , can use (17), and ensuring the exploration-exploitation balance adjusts with iteration numbers, can use (19). The algorithm parameters, such as the number of agents/salps, Max_Iter , and archive size, are illustrated in the flowchart depicted in Figure 2.

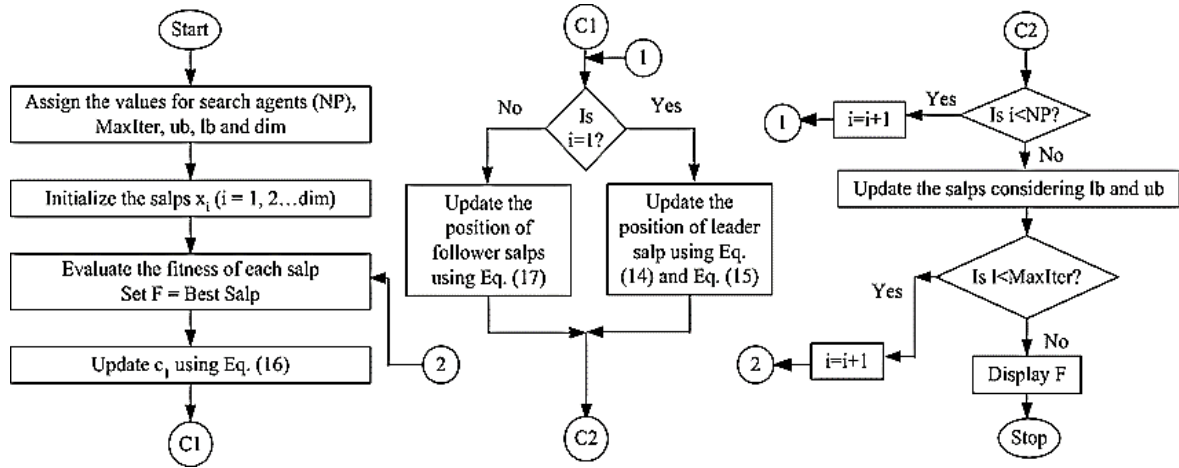


Figure 2. Flowchart of SSA

4. RESULTS AND DISCUSSION

Positive results have been obtained when optimizing PID controllers in the salp swarm algorithm (SSA) is used to control the load frequency (LFC) in a parallel two-area power system. Analyzing dynamic system responses to a 1 percent step load perturbation at $t = 0$ s, the study compares the ideal controller's performance with the SSA-optimized integral controllers.

4.1. Transient characteristics

The study introduces a step load perturbation of one percent at $t = 0$ s using SSA-optimized controllers and analyses the transient characteristics of the system. As Figure 3 illustrates, the SSA-optimized integral controller outperforms the ideal controller in terms of peak overshoot reduction and settling time acceleration.

4.2. Dynamic frequency deviation responses

The dynamic frequency deviation responses to a 1% step load perturbation in area 1 at $t = 0$ s in a system with and without an AC line are shown in detail in Figures 3 and 4. Both f_1 and f_2 show notable gains compared to the closed-loop system output of ideal controllers, with a 20.35 percent enhancement for f_1 and a 10.78 percent improvement for f_2 .

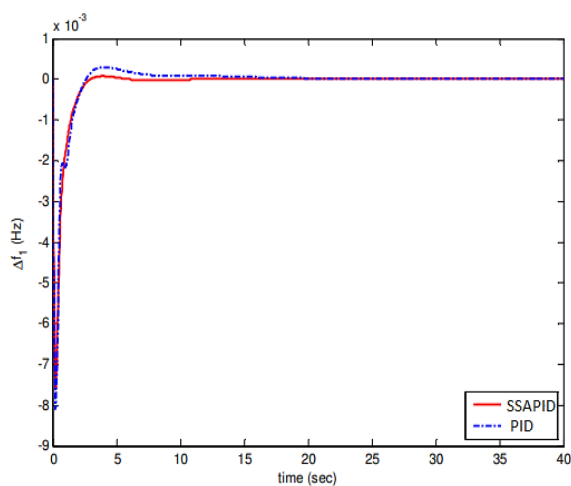


Figure 3. Demonstrates, for a 1% change in area -1, the variation in area -1's frequency when using AC-DC parallel tie wires

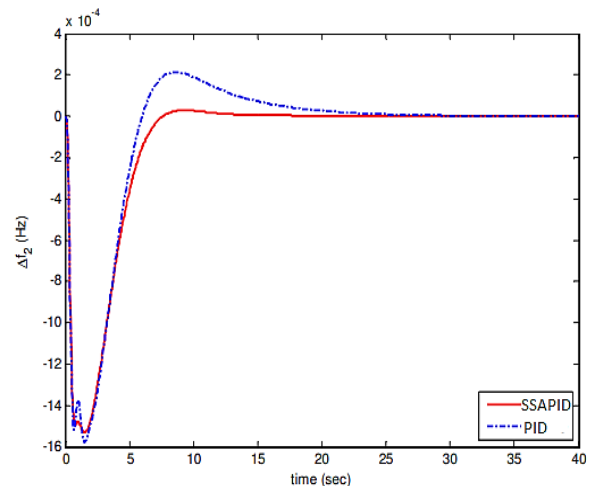


Figure 4. The frequency of area -2 changes with every 1% change in area -1 when using AC-DC parallel tie lines

4.3. Power deviations in tie-lines

In Figure 5, the variation in tie-line power over time is depicted under a consistent 1% step load perturbation. The SSA-optimized PID controller is evident in substantially mitigating both overshoot and undershoot. Graphically, there is a notable 32.85% increase in undershoot and a remarkable 88.33% reduction in overshoot. Figure 5 displays the tie-line power deviations for the recommended SSA-designed PID/PI/I controllers. Furthermore, a comparison with an ideal output feedback controller designed for a system is provided that is similar. Improved settling times are demonstrated by the PID, PI, and I controllers, which have gains of 66.46%, 65.23%, and 12.5%, respectively.

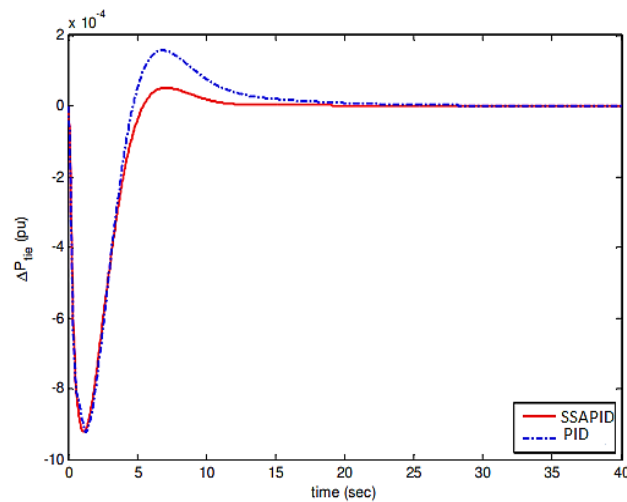


Figure 5. Variation in area -1's tie line power with a movement of 1-3 percent using AC-DC parallel tie lines

4.4. Transient response specifications

Table 1 provides a comprehensive list of transient response parameters, encompassing settling time (T_s), maximum overshoot (MOS), and maximum undershoot (MUS). The remarkable effectiveness of the proposed SSA algorithm is evident, as the SSA-PID controller consistently outperforms the PID controller across all specifications. The superiority of the SSA algorithm over other optimization methods can be attributed to several factors, notably demonstrated through the consistent outperformance of the SSA-PID controller.

Table 1. Short-term system dynamic response measurements

Algorithm	Response	MPUS,Hz	MPOS,Hz	T_s ,s
SSA	ΔF_1	3.41×10^{-3}	6.64×10^{-4}	6.48
PID		5.36×10^{-3}	12.53×10^{-4}	7.89
SSA	ΔF_2	8.11×10^{-4}	1.80×10^{-4}	14.5
PID		19.68×10^{-4}	4.13×10^{-4}	14.9
SSA	ΔP_{tie}	3.27×10^{-4}	6.42×10^{-5}	14.7
PID		7.49×10^{-4}	11.55×10^{-5}	15.8

5. CONCLUSION

This paper presents the self-adaptive social spider algorithm (SSA) as a potentially effective way to improve PID controllers in multi-area hybrid renewable power systems with nonlinear dynamics. The combination of renewable energy sources and system nonlinearities present difficult issues that can be resolved using the SSA-PID controller, making it a useful tool for enhancing system dynamics and stability. Its effectiveness in handling the complexities of hybrid renewable power systems is demonstrated by simulation studies, providing a sustainable answer to the demands of the modern energy market. These results highlight how critical it is to use cutting-edge optimization techniques like SSA-PID in order to satisfy the pressing need for dependable and effective renewable energy integration. Adopting such strategies can help to actively advance the creation of robust and responsive energy systems. Subsequent investigations




ought to concentrate on improving SSA-based techniques and investigating their suitability for use in various diverse energy landscapes.

REFERENCES




- [1] H. M. Hasanien, "Whale optimisation algorithm for automatic generation control of interconnected modern power systems including renewable energy sources," *IET Generation, Transmission & Distribution*, vol. 12, no. 3, pp. 607–614, 2017, doi: 10.1049/iet-gtd.2017.1005.
- [2] I. Altawil, M. A. Momani, M. A. Al-Tahat, R. Al Athamneh, M. A. Al-Saadi, and Z. Albataineh, "Optimization of fractional order PI controller to regulate grid voltage connected photovoltaic system based on slap swarm algorithm," *International Journal of Power Electronics and Drive Systems (IJPEDS)*, vol. 14, no. 2, p. 1184, 2023, doi: 10.11591/ijpeds.v14.i2.pp1184-1200.
- [3] B. Ahmadi and R. Çağlar, "Determining the Pareto front of distributed generator and static VAR compensator units placement in distribution networks," *International Journal of Electrical and Computer Engineering (IJECE)*, vol. 12, no. 4, p. 3440, 2022, doi: 10.11591/ijece.v12i4.pp3440-3453.
- [4] M. H. Mohamedy Ali, M. M. Sayed Mohamed, N. M. Ahmed, and M. B. A. Zahran, "Comparison between P&O and SSO techniques based MPPT algorithm for photovoltaic systems," *International Journal of Electrical and Computer Engineering (IJECE)*, vol. 12, no. 1, p. 32, 2022, doi: 10.11591/ijece.v12i1.pp32-40.
- [5] M. A. Shawqi, M. H. Abdallah, and I. A. Nassar, "Impact of on-grid solar energy generation system on low voltage ride through capability," *International Journal of Power Electronics and Drive Systems (IJPEDS)*, vol. 13, no. 1, p. 488, 2022, doi: 10.11591/ijpeds.v13.i1.pp488-499.
- [6] A. Kumar GB, S. Shivashankar, and K. Keshavamurthy, "Design and control of grid-connected solar-wind integrated conversion system with DFIG supplying three-phase four-wire loads," *International Journal of Power Electronics and Drive Systems (IJPEDS)*, vol. 12, no. 2, p. 1150, 2021, doi: 10.11591/ijpeds.v12.i2.pp1150-1161.
- [7] A. F. Mirza, M. Mansoor, Q. Ling, B. Yin, and M. Y. Javed, "A Salp-Swarm Optimization based MPPT technique for harvesting maximum energy from PV systems under partial shading conditions," *Energy Conversion and Management*, vol. 209, p. 112625, Apr. 2020, doi: 10.1016/j.enconman.2020.112625.
- [8] A. M. Elsherbiny, A. S. Nada, and M. K. Ahmed, "Smooth transition from grid to standalone solar diesel mode hybrid generation system with a battery," *International Journal of Power Electronics and Drive Systems (IJPEDS)*, vol. 10, no. 4, p. 2065, 2019, doi: 10.11591/ijpeds.v10.i4.pp2065-2075.
- [9] M. B S and B. Basavaraja, "ANFIS based hybrid solar and wave generator for distribution generation to grid connection," *International Journal of Power Electronics and Drive Systems (IJPEDS)*, vol. 10, no. 1, p. 479, 2019, doi: 10.11591/ijpeds.v10.i1.pp479-485.
- [10] K. Emami, T. Fernando, H. H.-C. Iu, B. D. Nener, and K. P. Wong, "Application of Unscented Transform in Frequency Control of a Complex Power System Using Noisy PMU Data," *IEEE Transactions on Industrial Informatics*, vol. 12, no. 2, pp. 853–863, 2016, doi: 10.1109/tii.2015.2491222.
- [11] H. L. Zeynelgil, A. Demirören, and N. S. Şengör, "Load frequency control for power system with reheat steam turbine and governor deadband non-linearity by using neural network controller," *European Transactions on Electrical Power*, vol. 12, no. 3, pp. 179–184, 2002, doi: 10.1002/etep.4450120303.
- [12] C.-F. Juang and C.-F. Lu, "Load-frequency control by hybrid evolutionary fuzzy PI controller," in *IEE Proceedings - Generation, Transmission and Distribution*, 2006, vol. 153, no. 2, p. 196. doi: 10.1049/ip-gtd:20050176.
- [13] H. A. Yousef, K. AL-Kharusi, M. H. Albadi, and N. Hosseinzadeh, "Load Frequency Control of a Multi-Area Power System: An Adaptive Fuzzy Logic Approach," *IEEE Transactions on Power Systems*, vol. 29, no. 4, pp. 1822–1830, 2014, doi: 10.1109/tpwrs.2013.2297432.
- [14] S. R. Khuntia and S. Panda, "Simulation study for automatic generation control of a multi-area power system by ANFIS approach," *Applied Soft Computing*, vol. 12, no. 1, pp. 333–341, 2012, doi: 10.1016/j.asoc.2011.08.039.
- [15] S. Patra, S. Sen, and G. Ray, "Design of Robust Load Frequency Controller: H_∞ Loop Shaping Approach," *Electric Power Components and Systems*, vol. 35, no. 7, pp. 769–783, 2007, doi: 10.1080/15325000601175140.
- [16] K. Vrdoljak, N. Perić, and I. Petrović, "Sliding mode based load-frequency control in power systems," *Electric Power Systems Research*, vol. 80, no. 5, pp. 514–527, 2010, doi: 10.1016/j.epr.2009.10.026.
- [17] W. Tan and Z. Xu, "Robust analysis and design of load frequency controller for power systems," *Electric Power Systems Research*, vol. 79, no. 5, pp. 846–853, 2009, doi: 10.1016/j.epr.2008.11.005.
- [18] H. M. Hasanien and S. M. Muyeen, "Design Optimization of Controller Parameters Used in Variable Speed Wind Energy Conversion System by Genetic Algorithms," *IEEE Transactions on Sustainable Energy*, vol. 3, no. 2, pp. 200–208, 2012, doi: 10.1109/tste.2012.2182784.
- [19] G. Islam, S. M. Muyeen, A. Al-Durra, and H. M. Hasanien, "RTDS implementation of an improved sliding mode based inverter controller for PV system," *ISA Transactions*, vol. 62, pp. 50–59, 2016, doi: 10.1016/j.isatra.2015.10.022.
- [20] H. M. Hasanien and M. Matar, "Water cycle algorithm-based optimal control strategy for efficient operation of an autonomous microgrid," *IET Generation, Transmission & Distribution*, vol. 12, no. 21, pp. 5739–5746, 2018, doi: 10.1049/iet-gtd.2018.5715.
- [21] D. Lakshmi, A. P. Fathima, and R. Muthu, "Simulation of the Two - Area Deregulated Power System using Particle Swarm Optimization," *International Journal on Electrical Engineering and Informatics*, vol. 8, no. 1, pp. 93–107, 2016, doi: 10.15676/ijeii.2016.8.1.7.
- [22] L. Dhandapani, P. Abdulkareem, and R. Muthu, "Two-area load frequency control with redox flow battery using intelligent algorithms in a restructured scenario," *Turkish Journal Of Electrical Engineering & Computer Sciences*, vol. 26, pp. 330–346, 2018, doi: 10.3906/elk-1512-298.
- [23] F. Daneshfar and H. Bevrani, "Load–frequency control: a GA-based multi-agent reinforcement learning," *IET Generation, Transmission & Distribution*, vol. 4, no. 1, p. 13, 2010, doi: 10.1049/iet-gtd.2009.0168.
- [24] H. Gozde and M. C. Taplamacioglu, "Automatic generation control application with craziness based particle swarm optimization in a thermal power system," *International Journal of Electrical Power & Energy Systems*, vol. 33, no. 1, pp. 8–16, 2011, doi: 10.1016/j.ijepes.2010.08.010.
- [25] D. Lakshmi, R. Zahira, C. N. Ravi, G. Ezhilarasi, and C. Nayanatara, "Flower Pollination Algorithm in DPS Integrated DFIG for Controlling Load Frequency," in *2020 International Conference on Power, Energy, Control and Transmission Systems (ICPECTS)*, 2020. doi: 10.1109/icpects49113.2020.9337017.

BIOGRAPHIES OF AUTHORS






Pushpa Sreenivasan    is a research scholar in Electrical and Electronics Engineering Department at the Academy of Maritime Education (AMET) University, Tamilnadu, India. She has 18 years of teaching experience. She received her B.E., degree in Electrical and Electronics Engineering from Madras University in the year 2003, M.E., degree in Power System Engineering in Anna University, Tamilnadu, India, in 2009, respectively. She is currently an assistant professor, at Panimalar Engineering College, Tamilnadu, India. Her research interests include the field of power system, renewable energy, electrical machines, control system, and microgrid. She is a life member in professional bodies like IAENG. She got an organizer award in green energy SDG. She can be contacted at email: puvehava@gmail.com.






Lakshmi Dhandapani    is a professor of Department of Electrical and Electronics Engineering, Academy of Maritime Education and Training, deemed to be University, Chennai, Tamil Nādu, India. She has more than 23 years of expertise in the field of power system. She has guided more than 30 UG students, 15 PG students and 5 research scholars. She has published 11 book chapters and 6 books, 46 articles in SCI and Scopus indexed journals and nearly 35 national level and international level conferences proceedings. She is a life member in professional bodies such as IEEE, IEI, IAENG, and InSc. She is a star organizer in IGEN Energathon-2023 Marathon, a new world record on longest conference. Her areas of interest are power system operation and control, soft computing renewable energy systems, microgrid, and electrical machines. She can be contacted at email: lakshmiee@gmail.com.






Shanthi Natarajan    is an assistant professor in Electrical and Electronic Engineering Department, Sri Sai Ram Institute of Technology, Chennai, India since 2010. She received B.E. degree in Electrical and Electronics Engineering from Madras University, Tamil Nadu in 1998 and the M.E. degree in Power Electronic and Drives from Madha Engineering College, Anna University, India in 2008; and currently pursuing Ph.D. in Power Electronics from Anna University, Tamil Nadu, India. She is also a member of IEI and IEEE professional societies. Her research interests include the field of power electronics, motor drives, and photovoltaic power systems. She can be contacted at email: shanthi.eee@sairamit.edu.in.



Arul Doss Adaikalam    received B.E. degree in Electrical and Electronics Engineering and M.E. degree in Power System Engineering, both from Anna University, Chennai in 2005 and 2009, respectively. He received the Ph.D. degree in Electrical Engineering from Anna University, Chennai, in 2020. He has 14 years of work experience in the field of teaching from various reputed academic organizations across Tamil Nadu, India, since 2009. He is currently working as assistant professor in Chennai Institute of Technology, Chennai. He is the life member of Indian Society for Technical Education, and other Professional Societies. He can be contacted at email: iadaickalam@gmail.com.



Amudhapriya Sivakumar    is an assistant professor in Electrical & Electronic Engineering Department, Panimalar Engineering College, India since 2019. She received the B.E. degree in Electrical and Electronics Engineering from Anna University in 2010 and the M.E., degree in Power Electronics, at St. Peters University, Tamilnadu, India, in 2019, respectively. Her research interests include the field of power electronics, motor drives industrial applications, industrial electronics, photovoltaic power systems, digital design front-end RTL logic design, and field programmable gate array applications. She can be contacted at email: amudhapriya.21@gmail.com.